

Thermophysical properties of liquid carbon dioxide under shock compressions: Quantum molecular dynamic simulations

Cong Wang¹ and Ping Zhang^{1,2,*}

¹*LCP, Institute of Applied Physics and Computational Mathematics,
P.O. Box 8009, Beijing 100088, People's Republic of China*

²*Center for Applied Physics and Technology,
Peking University, Beijing 100871, People's Republic of China*

Abstract

Quantum molecular dynamic simulations are introduced to study the dynamical, electrical, and optical properties of carbon dioxide under dynamic compressions. The principal Hugoniot derived from the calculated equation of states is demonstrated to be well accordant with experimental results. Molecular dissociation and recombination are investigated through pair correlation functions, and decomposition of carbon dioxide is found to be between 40 and 50 GPa along the Hugoniot, where nonmetal-metal transition is observed. In addition, the optical properties of shock compressed carbon dioxide are also theoretically predicted along the Hugoniot.

PACS numbers: 65.20.De, 64.30.Jk, 51.70.+f, 31.15.xv

*Corresponding author; zhang_ping@iapcm.ac.cn

I. INTRODUCTION

Knowledge of pressure-induced transformations for materials under extreme conditions, which requires accurate understandings of the thermophysical properties into new and complex region, has gained much interest in a large number of scientific and technological domains [1]. Carbon dioxide (CO_2) is one kind of the most important molecules in planetary science and chemical (or explosive) process. For instance, the magnetic fields and evolution of planets are closely related to the equation of states (EOS) and electrical properties of planetary interiors [2, 3], which are composed of species containing C, H, N, O, etc.; Chemical reactions of carbonaceous molecules (such as CO_2 , CO), nitrogen (N_2), oxygen (O_2) and their mixture at high densities and temperatures are focused due to their presence in reacted chemical explosives [4–7]. From these aspects, clearly, an accurate description of thermodynamical properties of CO_2 at high pressures and temperatures is fundamental and proves itself to be indispensable for developing realistic models of planetary interiors and reacted explosives.

Solid phase diagram of carbon dioxide up to 80 GPa and molecular-nonmolecular transition have already been probed through diamond-anvil cells and confocal micro-Raman spectroscopy [8–11]. Solid specimens were reported to be stable until the formation of *a*-carbonia (an amorphous extended phase), which can only be revealed around 50 GPa at elevated temperature or above 65 GPa at ambient temperature [11]. Here, we concentrate on liquid specimens, which were first single shocked to 29 GPa and double-shocked to 56 GPa by Schott [12], then single shocked to 71 GPa by Nellis *et al.* [13] using a two-stage light-gas gun. Theoretically, intermolecular potential method was applied to study the EOS of CO_2 under dynamic compressions, where the onset of decomposition was reported to be around 30 GPa (4500 K, $17 \text{ cm}^3/\text{mol}$) along the Hugoniot [13]. Despite that the predicted EOS were in accord with experimental data, the electronic structure, which has been proved to be important in determining the dynamical, electrical, and optical properties of molecular fluids under extreme conditions [14–16], is still lacking due to the intrinsic approximations of this method.

On the other hand, quantum molecular dynamic (QMD) simulations, where quantum-mechanical treatments are executed by combining classical molecular dynamics for the ions and density functional theory (DFT) for electrons, have already been proved to be successful

in describing the thermodynamical properties of mono atomic molecules (He) [17], diatomic molecules (H_2 , N_2 , O_2) [18–20], and hydrocarbons (C_6H_6) [16] under extreme conditions. A fully quantum-mechanical description of CO_2 under shock compressions is highly recommended to be presented and understood because of the following aspects: (i) CO_2 undergoes dramatic transformations under shock compressions, such as dissociation and recombination of molecules, during which carbonaceous molecules combined with oxygen (O_2) might be produced, and electron spin polarization should be seriously considered at this stage due to the fact that spin-triplet state governs the ground state of oxygen [21]; (ii) Electrical conductivity of molecular fluid, where electronic structure is of dominance, can be greatly influenced by thermo-activated electronic states under extreme conditions; (iii) Temperature, which is an important parameter in experimental determination of EOS, is usually difficult to be measured because of the uncertainty in determining the optical intensity for ultraviolet part of the spectrum, and QMD simulations are powerful tools to provide predictions.

In the present work, DFT-based QMD simulations have been used to investigate thermophysical properties of CO_2 under extreme conditions. The EOS and pair correlation functions (PCF) are determined through QMD simulations at equilibrium. Dynamic conductivity $\sigma(\omega)$ is calculated by Kubo-Greenwood formula, from which the dc conductivity (σ_{dc}) is determined. Then, the dielectric function $\epsilon(\omega)$ and reflectivity are extracted. The rest of this paper is organized as follows. The simulation details are briefly described in Sec. II; The PCF, which is used to study the dissociation of CO_2 , and the Hugoniot curve are given in Sec. III A; In Sec. III B, nonmetal-metal transition and optical properties are discussed. Finally, we close our paper with a summary of our main results in Sec. IV.

II. COMPUTATIONAL METHOD

The Vienna Ab-initio Simulation Package (VASP) [22, 23], which was developed at the Technical University of Vienna, has been employed to perform simulations for carbon dioxide. The elements of our calculations consist of a series of volume-fixed supercells including N atoms, which are repeated periodically throughout the space. By involving Born-Oppenheimer approximation, electrons are quantum mechanically treated through plane-wave, finite-temperature (FT) DFT [24], where the electronic states are populated according to Fermi-Dirac distributions at temperature T_e . The exchange-correlation functional

is determined by generalized gradient approximation (GGA) with the parametrization of Perdew-Wang 91 [25]. The ion-electron interactions are represented by a projector augmented wave (PAW) pseudopotential [26]. Isokinetic ensemble (NVT) is adopted in present simulations, where the ionic temperature T_i is controlled by Noé thermostat [27], and the system is kept in local thermodynamical equilibrium by setting the electron (T_e) and ion (T_i) temperatures to be equal. Electron spin polarization has also been taken into account, due to the possible existence of oxygen molecules in shocked CO_2 .

The plane-wave cutoff energy is selected to be 600 eV so that the pressure is converged within 5% accuracy. Γ point and $4 \times 4 \times 4$ Monkhorst-Pack scheme \mathbf{k} points are used to sample the Brillouin zone in molecular dynamics simulation and electronic structure calculation, respectively, because EOS (conductivity) can only be modified within 5% (15%) for the selection of higher number of \mathbf{k} points. 81 atoms (27 CO_2 molecules) are included in the cubic supercell. The densities selected in our simulations range from 13 to $37.55 \text{ cm}^3/\text{mol}$ and temperatures between 218 and 10000 K, which highlight the regime of the Hugoniot. All the dynamic simulations are lasted for $3 \sim 6$ ps, and the time steps for the integrations of atomic motion are $0.5 \sim 1$ fs according to different densities (temperatures). Then, the subsequent 1 ps simulations are used to calculate EOS as running averages.

III. RESULTS AND DISCUSSION

A. EQUATION OF STATE

Accurate understandings of the electrical and optical properties of CO_2 depend on a precise description of dynamical properties, such as EOS. The EOS have been examined theoretically through the Rankine-Hugoniot equations, which follow from conservation of mass, momentum, and energy across the front of shock waves. The equations describe the locus of points in (E, P, V) -space satisfying the relation as follows:

$$E_1 - E_0 = \frac{1}{2}(P_1 + P_0)(V - V_0), \quad (1)$$

$$P_1 - P_0 = \rho_0 u_s u_p, \quad (2)$$

$$V_1 = V_0(1 - u_p/u_s), \quad (3)$$

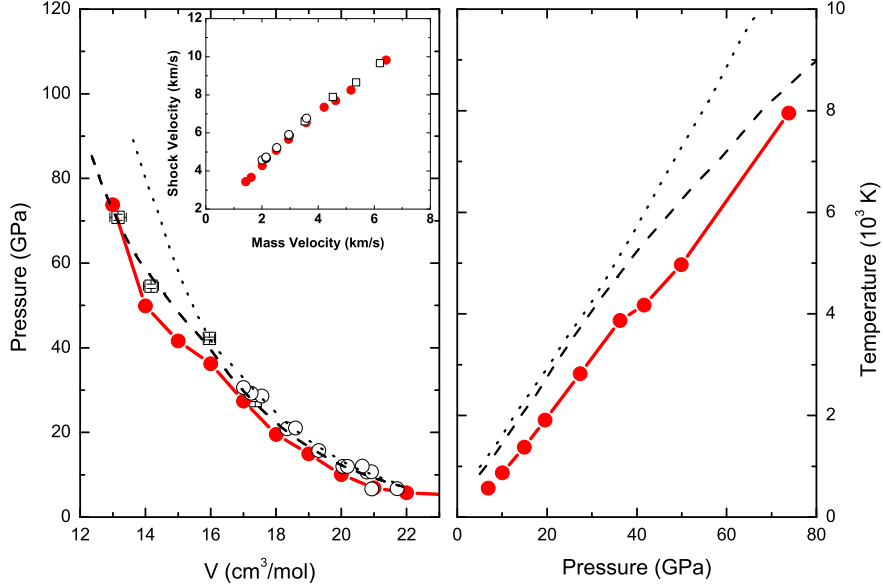


FIG. 1: (Color online) The P - V (left panel) and T - P (right panel) Hugoniot curves of shocked carbon dioxide. Inset is the (u_s, u_p) diagram. Here, filled red circles denote the present QMD results, while the dashed and dotted lines denote the intermolecular potential results [13] with and without accounting for molecular dissociation, respectively. The experimental data reported in Ref. [12] (open circles) and Ref. [13] (open squares) are also shown for comparison.

where E , P , V denote internal energy, pressure, volume, and subscripts 0 and 1 present the initial and shocked state, respectively. In Eqs. (2) and (3), u_s is the velocity of the shock wave and u_p corresponds to the mass velocity of the material behind the shock front. In the present work, the initial density of CO_2 is $\rho_0 = 1.17 \text{ g/cm}^3$ ($V_0 = 37.55 \text{ cm}^3/\text{mol}$) and the liquid specimen is controlled at a temperature of 218 K, where the internal energy is $E_0 = -22.95 \text{ eV/molecule}$. The initial pressure P_0 can be treated approximately as zero compared to the high pressure of shocked states along the Hugoniot. The Hugoniot points are obtained as follows: (i) smooth functions are used to fit the internal energy and pressure in terms of temperature at sampled density; (ii) then, Hugoniot points are derived from Eq. (1). The results are summarized in Table I.

Comparisons between our simulated Hugoniot curve and results from experimental measurement and intermolecular potential method are shown in Fig. 1 (left panel), where our

TABLE I: Hugoniot pressure and temperature points derived from QMD simulations at a series of molar volumes.

V (cm ³ /mol)	P (GPa)	T (K)
22	5.72	459
21	6.91	568
20	10.05	873
19	14.95	1374
18	19.53	1909
17	27.39	2821
16	36.24	3873
15	41.62	4175
14	49.89	4968
13	73.82	7955

results show good agreement with experiment. The QMD simulated pressure and temperature along the Hugoniot curve for carbon dioxide shows a systematic behavior, except for the region with a small break in slope around 40 to 50 GPa, where structural transitions characterize the EOS of molecular fluid. Although the P - V curve by intermolecular potential method is consistent with experiments, the predicted temperature remains too high compared with our calculations [see Fig. 1 (right panel)].

Dynamical properties and structural transitions of CO₂ under extreme conditions have been examined through PCF, which represents the possibility of finding a particle at a distance r from a reference atom. Figure 2 shows PCF and charge density distribution (at equilibrium) of four different molar volume points, and the structural transitions of CO₂ are clearly reflected by PCF. At low pressures [Fig. 2(a)], ideal molecular fluid is suggested by PCF distribution of C-O, which exhibits a main peak around 1.16 Å. With the increase of pressure along the Hugoniot, this main peak in C-O PCF reduces in amplitude and get broadened, which is attributed to the thermo-induced vibrations of C-O bonds around the equilibrium length. Dissociation of CO₂, which leads to soften behavior of the Hugoniot [see Fig. 1 (left panel)], has been found at about 40 to 50 GPa. It is indicated that carbon atoms tend to form connections between each other [Fig. 2(c)], then, with further increase

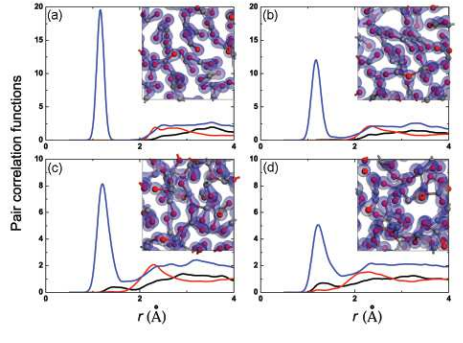


FIG. 2: (Color online) Calculated pair correlation function for C-O (blue line), C-C (black line), O-O (red line) at four densities of CO₂ along the Hugoniot. The atomic structure, where carbon and oxygen atoms are denoted by gray and red balls respectively, and the relative iso-surface of charge density (blue regimes) are also provided in the insets. (a) $V = 19 \text{ cm}^3/\text{mol}$, $T = 1374 \text{ K}$; (b) $V = 16 \text{ cm}^3/\text{mol}$, $T = 3873 \text{ K}$; (c) $V = 15 \text{ cm}^3/\text{mol}$, $T = 4175 \text{ K}$; (d) $V = 13 \text{ cm}^3/\text{mol}$, $T = 7955 \text{ K}$.

of pressure, hybrid C-C bonds (peak around 1.45 \AA , which lies between typical sp^3 and sp^4 hybrid C-C bond length), diatomic oxygen (peak around 1.23 \AA) and mono-atomic oxygen are formed in the shocked system [Fig. 2(d)]. Furthermore, we have examined the charge density difference between spin-up and spin-down electrons, which is as small as negligible, and the results suggest that electron spin polarization of the shock produced mono-atomic and diatomic oxygen are suppressed at this stage.

B. DYNAMIC CONDUCTIVITY

Great controversies have been raised since the detection of nonmetal-metal transition of such diatomic molecules as hydrogen and oxygen [28, 29] in isentropic compressions. The links between nonmetal-metal transition and dissociation of molecules under dynamic compression are of particular significance. Here, we examine the dynamic conductivity of CO₂ according to Kubo-Greenwood formula:

$$\sigma_1(\omega) = \frac{2\pi}{3\omega\Omega} \sum_{\mathbf{k}} w(\mathbf{k}) \sum_{j=1}^N \sum_{i=1}^N \sum_{\alpha=1}^3 [f(\epsilon_i, \mathbf{k}) - f(\epsilon_j, \mathbf{k})] \times |\langle \Psi_{j,\mathbf{k}} | \nabla_{\alpha} | \Psi_{i,\mathbf{k}} \rangle|^2 \delta(\epsilon_{j,\mathbf{k}} - \epsilon_{i,\mathbf{k}} - \hbar\omega), \quad (4)$$

where Ω is the volume of the supercell. The i and j summations range over N discrete bands included in the calculation. The α sum is over the three spatial directions. $f(\epsilon_i, \mathbf{k})$ describes

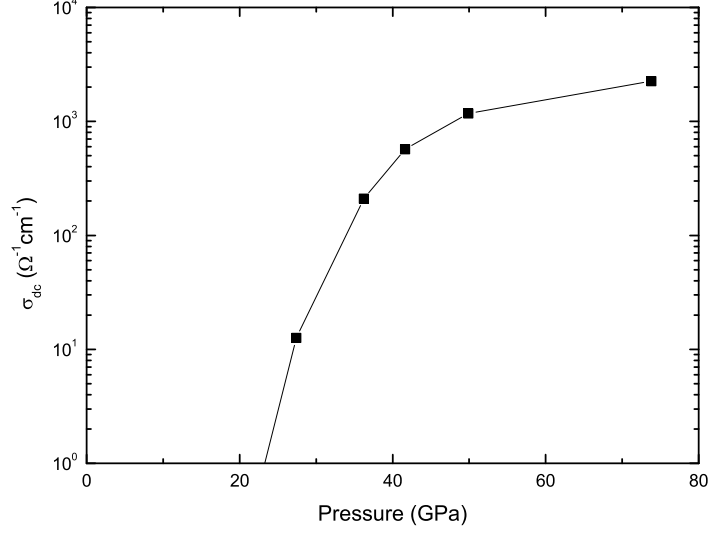


FIG. 3: Calculated dc conductivity of shocked carbon dioxide along the Hugoniot.

the occupation of the i th band, with the corresponding energy $\epsilon_{i,\mathbf{k}}$ and the wavefunction $\Psi_{i,\mathbf{k}}$ at \mathbf{k} . $w(\mathbf{k})$ is the \mathbf{k} -point weighting factor.

Along the Hugoniot, dynamic conductivity have been calculated as the average of thirty atomic snapshots at equilibrium. The dc conductivity (σ_{dc}), which follows the static limit ($\omega \rightarrow 0$) of $\sigma_1(\omega)$, is then extracted and plotted in Fig. 3. At pressures below 20 GPa, σ_{dc} can be neglected, and the results suggest an insulating molecular fluid. Thermal activation of conductivity is raised from 20 GPa, then metallization ($\sigma_{dc} > 1000 \text{ } \Omega^{-1}\text{cm}^{-1}$) of CO_2 , which is accompanied with dissociation of molecules, is reached at 40 to 50 GPa.

Emissivity of spectrum, which is closely related to optical reflectivity, is important in determining temperature in experiment. Optical reflectivity can be derived from dynamic conductivity. The imaginary part $\sigma_2(\omega)$ can be obtained from the Kramers-Kronig relation:

$$\sigma_2(\omega) = -\frac{2}{\pi}P \int \frac{\sigma_1(\nu)\omega}{\nu^2 - \omega^2} d\nu, \quad (5)$$

where P is the principal value of the integral. Then dielectric functions can be derived from the two parts of the conductivity:

$$\epsilon_1(\omega) = 1 - \frac{4\pi}{\omega} \sigma_2(\omega), \quad (6)$$

$$\epsilon_2(\omega) = \frac{4\pi}{\omega} \sigma_1(\omega). \quad (7)$$

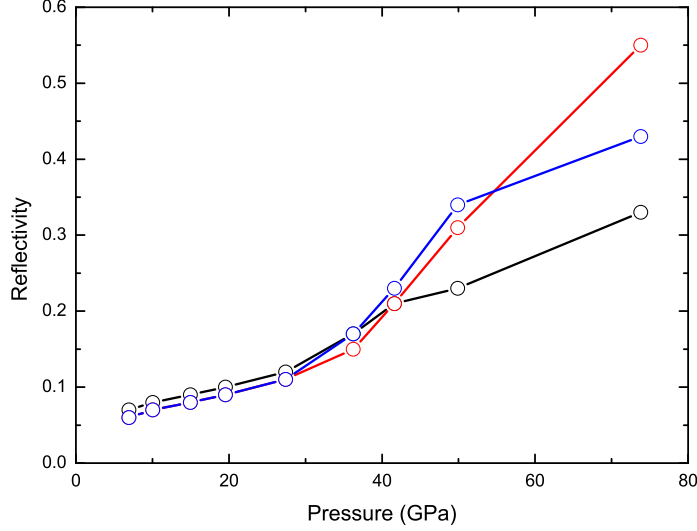


FIG. 4: (Color online) Optical reflectivity of shocked carbon dioxide for wavelengths of 404 (black line), 808 (red line), and 1064 nm (blue line) along the Hugoniot.

The real part $n(\omega)$ and the imaginary part $k(\omega)$ of the refraction index have the following relations with dielectric function:

$$n(\omega) = \sqrt{\frac{1}{2} [|\epsilon(\omega)| + \epsilon_1(\omega)]}, \quad (8)$$

$$k(\omega) = \sqrt{\frac{1}{2} [|\epsilon(\omega)| - \epsilon_1(\omega)]}. \quad (9)$$

The index of refraction is useful for evaluating optical properties such as the reflectivity $r(\omega)$ and absorption coefficient $\alpha(\omega)$:

$$r(\omega) = \frac{[1 - n(\omega)]^2 + k(\omega)^2}{[1 + n(\omega)]^2 + k(\omega)^2}. \quad (10)$$

We have examined the optical reflectance at three wavelengths (404, 808, and 1064 nm) spanning the visible spectrum, and the results are shown along the Hugoniot in Fig. 4, which clearly shows the pressure-induced change in reflectivity (from 0.05 to 0.35 ~ 0.55). For the pressure between 20 and 40 GPa, the increase in reflectance is retarded, then sharp increase exists around 40 to 50 GPa due to the nonmetal-metal transition. The results could be inspected by future experiments.

IV. CONCLUSION

In summary, we have studied the thermodynamical properties of carbon dioxide under extreme conditions. The EOS obtained from QMD simulations are used to determine the Hugoniot curve, which shows good agreement with available experimental data. Our calculations indicate that decomposition of carbon dioxide begins at 40 to 50 GPa along the Hugoniot, where carbon atoms intend to form connections between each other, then diatomic and monoatomic oxygen are produced. The nonmetal-metal transition, as well as the change in optical reflectance, are also found in the present work.

Acknowledgments

This work was supported by NSFC under Grants No. 90921003 and No. 60776063.

-
- [1] R. Ernstorfer, M. Harb, C. T. Hebeisen, G. Sciaini, T. Dartigalongue, and R. J. D. Miller, *Science* **323**, 1033 (2009).
 - [2] M. L. Elert, S. V. Zybin, and C. T. White, *J. Chem. Phys.* **118**, 9795 (2003).
 - [3] D. J. Stevenson, *Annu. Rev. Earth Planet Sci.* **14**, 257 (1982).
 - [4] R. W. Armstrong, *Rev. Adv. Mater. Sci.* **19**, 13 (2009).
 - [5] S. C. Baber and A. M. Dean, *J. Chem. Phys.* **60**, 307 (1974).
 - [6] W. O. Davies, *J. Chem. Phys.* **43**, 2809 (1965).
 - [7] Z. Zhang and Z. Duan, *J. Chem. Phys.* **122**, 214507 (2005).
 - [8] V. M. Giordano, F. Datchi, and A. Dewaele, *J. Chem. Phys.* **125**, 054504 (2006).
 - [9] O. Tschauner, H. Mao, and R. J. Hemley, *Phys. Rev. Lett.* **87**, 075701 (2001).
 - [10] J. A. Montoya, R. Rousseau, M. Santoro, F. Gorelli, and S. Scandolo, *Phys. Rev. Lett.* **100**, 163002 (2008).
 - [11] A. Sengupta and C. Yoo, *Phys. Rev. B* **80**, 014118 (2009).
 - [12] G. L. Schott, *High Press. Res.* **6**, 187 (1991).
 - [13] W. J. Nellis, A. C. Mitchell, F. H. Ree, M. Ross, N. C. Holmes, R. J. Trainor, and D. J. Erskine, *J. Chem. Phys.* **95**, 5268 (1991).
 - [14] M. Bastea, C. Mitchell, and W. J. Nellis, *Phys. Rev. Lett.* **86**, 3108 (2001).

- [15] C. Wang and P. Zhang, J. Chem. Phys. **132**, 154307 (2010).
- [16] C. Wang and P. Zhang, J. Appl. Phys. **107**, 083502 (2010).
- [17] B. Militzer, Phys. Rev. Lett. **97**, 175501 (2006).
- [18] V. Recoules, F. Lambert, A. Decoster, B. Canaud, and J. Cl  rouin, Phys. Rev. Lett. **102**, 075002 (2009).
- [19] S. Mazevet, J. D. Kress, L. A. Collins, and P. Blottiau, Phys. Rev. B **67**, 054201 (2003).
- [20] B. Militzer, F. Gygi, and G. Galli, Phys. Rev. Lett. **91**, 265503 (2003).
- [21] K. Sugimori, T. Oda, H. Nagao, I. Hamada, S. Kagayama, M. Geshi, H. Nagara, K. Kusakabe, and N. Suzuki, J. Phys.: Condens. Matter **19**, 365211 (2007).
- [22] G. Kresse and J. Hafner, Phys. Rev. B **47**, R558 (1993).
- [23] G. Kresse and J. Furthm  ller, Phys. Rev. B **54**, 11169 (1996).
- [24] T. Lenosky, S. Bickham, J. Kress, and L. Collins, Phys. Rev. B **61**, 1 (2000).
- [25] J. P. Perdew, *Electronic Structure of Solids* (Akademie Verlag, Berlin, 1991).
- [26] P. E. Bl  chl, Phys. Rev. B **50**, 17953 (1994).
- [27] S. Nos  , J. Chem. Phys. **81**, 511 (1984).
- [28] M. Bastea, Phys. Rev. Lett. **92**, 129601 (2004).
- [29] R. Chau, A. C. Mitchell, R.W. Minich, and W. J. Nellis, Phys. Rev. Lett. **92**, 129602 (2004).